



Original article

Dexpanthenol improved stem cells against cisplatin-induced kidney injury by inhibition of TNF- α , TGF β -1, β -catenin, and fibronectin pathways



Khalifa El-Dawy^a, Nashwa Barakat^{b,*}, Hala Ali^a, Ikhlas A. Sindi^{c,d}, Heba M. Adly^e, Saleh A.K. Saleh^{f,g}

^a Biochemistry Dept., Faculty of Veterinary Medicine, Zagazig University, Zagazig, Egypt

^b Urology and Nephrology Center, Mansoura University, Mansoura, Egypt

^c Preparatory Year Program, Batterjee Medical College, Jeddah 21442, Saudi Arabia

^d Department of Biology, Faculty of Science, King Abdulaziz University, Jeddah, Saudi Arabia

^e Community Medicine and Pilgrims Healthcare Department, Faculty of Medicine, Umm Al-Qura University, Makkah 21955, Saudi Arabia

^f Biochemistry Department, Faculty of Medicine, Umm Al-Qura University, Makkah 21955, Saudi Arabia

^g Oncology Diagnostic Unit, Faculty of Medicine, Ain Shams University, Cairo 11435, Egypt

ARTICLE INFO

Article history:

Received 16 July 2023

Revised 30 July 2023

Accepted 3 August 2023

Available online 9 August 2023

Keywords:

Nephrotoxicity

Dexpanthenol

ADMSCs

Cisplatin

ABSTRACT

Introduction: Cisplatin interacts with DNA and induces an immunological response and reactive oxygen species, which are nephrotoxic mediators. Stem cells self-renew through symmetric divisions and can develop into other cell types due to their multipotency. Dexpanthenol has been proven to protect against renal injury.

Aim: This study aims to demonstrate that dexpanthenol could improve the effect of adipose-derived mesenchymal stem cells (ADMSC) against cisplatin-induced acute kidney injury.

Methods: Sixty male Sprague-Dawley rats were divided into 5 groups (N = 12): control, cisplatin, cisplatin & dexpanthenol, cisplatin & ADMSC, and cisplatin & dexpanthenol & ADMSCs. On the 5th day following cisplatin injection, half the rats in each group were sacrificed, and the other half were sacrificed on the 12th day. Histopathological examination, molecular studies (IL-6, Bcl2, TGF β -1, Caspase-3, Fibronectin, and β -catenin), antioxidants (superoxide dismutase and catalase), and renal function were all investigated.

Results: In contrast to cisplatin group, the dexpanthenol and ADMSCs treatments significantly decreased renal function and oxidative stress while significantly enhancing antioxidants. Dexpanthenol improved stem cells by significantly down-regulating caspase-3, IL-6, TGF- β 1, Fibronectin, and β -catenin and significantly up-regulating Bcl2 and CD34, which reversed the cisplatin effect.

Conclusion: Dexpanthenol enhanced ADMSCs' ability to protect against cisplatin-induced AKI by decreasing inflammation, apoptosis, and fibrosis.

© 2023 The Author(s). Published by Elsevier B.V. on behalf of King Saud University. This is an open access article under the CC BY-NC-ND license (<http://creativecommons.org/licenses/by-nc-nd/4.0/>).

1. Introduction

Acute kidney injury (AKI) caused an abrupt decline in renal function as well as waste product accumulation. When administered as chemotherapy for different malignancies, cisplatin damages renal tubular tissue and impairs kidney function by accumulating platinum inside the kidney, so it contributes to different patterns of nephrotoxicity and renal failure. The segment 3 (S3) region of the outer medulla is selectively damaged by cisplatin in the proximal tubules (Ghosh, 2019). The nephrotoxicity caused by cisplatin is caused by a complex mechanism that includes apoptosis, oxidative stress, proximal tubule injury, inflammatory reactions, and vascular injury (Barakat et al., 2021). By generating

* Corresponding author.

E-mail addresses: KAMohamed@vet.zu.edu.eg (K. El-Dawy), nashwab2006@mans.edu.eg (N. Barakat), h.ali23@vet.zu.edu.eg (H. Ali), ikhlas.sindi@bmc.edu.sa (I.A. Sindi), hmhasan@uqu.edu.sa (H.M. Adly), saabdrabou@uqu.edu.sa (S.A.K. Saleh).

Peer review under responsibility of King Saud University.



Production and hosting by Elsevier

<https://doi.org/10.1016/j.sjbs.2023.103773>

1319-562X/© 2023 The Author(s). Published by Elsevier B.V. on behalf of King Saud University.

This is an open access article under the CC BY-NC-ND license (<http://creativecommons.org/licenses/by-nc-nd/4.0/>).

covalent adducts between specific DNA bases and the platinum molecule, cisplatin interacts with DNA to cause cell cytotoxicity. In addition, reactive oxygen species (ROS), which are mediators of nephrotoxicity, and an immunological response were generated by cisplatin (Tang et al., 2021).

Dexpanthenol is a derivative of pantothenic acid. In the tissues, dexpanthenol increased antioxidants. As a result, it is crucial in the defense against inflammation and oxidative stress. Dexpanthenol has also been demonstrated to play a protective role against renal failure in numerous experimental models (Zhao et al., 2022).

Furthermore, the fast developing field of regenerative medicine is supported by numerous studies that have shown stem cells may replace injured or lost differentiated cells in a variety of tissues (Wong, 2021). Stem cells may self-renew through symmetric divisions and, depending on their multipotency, have the capacity to develop into different cell types. Mesenchymal stem cells (MSCs) can provide therapeutic benefits for AKI. MSCs have been extracted from a variety of tissues, including skin, adipose tissue, and placenta. Due to the simplicity of getting samples during surgical procedures like liposuction surgeries, adipose tissue is an attractive choice among all of these tissues for obtaining the cells required for clinical investigations (Alajez et al., 2018). So, this study aims to demonstrate that dexpanthenol could improve the effect of adipose-derived mesenchymal stem cells (ADMSC) against cisplatin-induced acute kidney injury.

2. Methods

2.1. Culture media preparation

In 50 ml falcon tubes, Dulbecco's modified Eagle's medium (DMEM) was aliquoted under laminar airflow and kept at 2 °C. Foetal bovine serum (FBS) was aliquoted into 15 ml falcon tubes after being deactivated at 56 °C for 20 min. Penicillin/streptomycin, an antibiotic, was initially frozen at -20 °C, thawed in a water bath, and then divided into 15 ml falcon tubes with a volume of 5 ml each. It was then again stored at -20 °C. After filtering, the tubes were heated in a water bath to 37 °C (Rafat et al., 2019).

2.2. ADMSCs preparation

A male Sprague-Dawley rat was used to extract ADMSCs. Small pieces of fat were cut and centrifuged by a Hitachi-koki centrifuge (211835, China) for 10 min at 2000 rpm after the paragonadal fat was extracted from the rat and placed in phosphate-buffered saline (PBS). The fat was then placed inside collagenase I 0.075% for 1 h at 37 °C to finish the digestion process before being centrifuged for 10 min at 2000 rpm. The generated supernatant was discarded, the pellet was resuspended in PBS, and it was centrifuged once more at 2000 rpm for 10 min. The pellet was resuspended in DMEM supplemented with 10% FBS and then transferred to a tissue culture flask and cultured in a 5% CO₂ incubator BJPX-C-Biobase (BJPX-C160D, China). Until the cells reached 70–80% confluence, the media was changed twice a week. The cells were subsequently given 0.25% trypsin and 1 mM EDTA (Thermo, USA) for 3 min. ADMSCs had a 1:3 split ratio modification. Cells were utilized after the third passage (Azandeh et al., 2012).

2.3. Flow cytometry evaluation

The cells were treated for 30 min at 25 °C in the dark with the phycoerythrin (PE)-conjugated CD90 and FITC-conjugated CD34 antibodies after being washed twice with PBS and aliquoted at a concentration of (1x10⁶/ml). After PBS washing, labelled cells were

analyzed with a flow cytometer (B53001, CytoFLEX V4-B5-R3, Beckman Coulter, USA) (Salehinejad et al., 2012).

2.4. Labeling of MSCs by BrdU

Mesenchymal stem cells stained with BrdU labeling according to Luo et al. (2017) and transplanted. A 10 µL of 10 mM BrdU was diluted in 10 ml of 37 °C tissue culture medium to make a 10 µM labeling solution. The cells were trypsinized, counted, and collected in sterile tubes. The culture medium from cells was removed and replaced with BrdU labeling solution. Then, the cells were incubated at 37 °C for 2 h. The labeling solution was removed and washed two times with PBS. Finally, the cells were washed twice with complete growth medium and became ready for transplantation.

2.5. Experimental animals

Sixty male Sprague-Dawley rats weighing between 180 and 220 g were used. The animals were fed a standard diet, had unlimited access to water, and had a 12-h light/12-h dark cycle.

2.6. Study design

The Sixty rats were distributed in five groups (N = 12): Group I (normal), Group II (Cisplatin): Normal rats were injected intraperitoneally with 6 mg/kg body weight of cisplatin (a liquid vial was purchased from Khandelwal Laboratories Pvt. Ltd.) (Barakat et al., 2021), Group III (Cisplatin & dexpanthenol): Normal rats received daily injections of 500 mg/kg dexpanthenol (a liquid vial was purchased from American Regent, Inc.) intraperitoneally after receiving a single dose of 6 mg/kg cisplatin intraperitoneally (Uysal et al., 2017), Group IV (Cisplatin & Stem cells): Rats were injected with the previous dose of cisplatin and after a day, the rats were injected intravenously by 0.2 ml culture media containing 1 × 10⁶ MSCs, Group V (Cisplatin & Dex & MSCs): as group III with the MSCs injection as group IV. Urine samples were obtained for the microalbuminuria (MAU) test prior to the sacrifice of each group. Six rats were sacrificed at 5 and 12 days from the beginning of the experiment, and samples of blood and renal tissues were collected.

2.7. Biochemical evaluations

Architect analyzer (c4000, Abbott Diagnostics, Germany) measured serum creatinine (SCr) and blood urea nitrogen (BUN) according to Koga et al. (2012). In the urine samples, MAU was also measured according to Cambiaso et al. (1988). The urine samples were mixed with anti-human albumin goat antiserum, and agglutination was caused by the antigen-antibody reaction. The turbidity was measured at 340 nm and 700 nm.

2.8. Assay of oxidative stress and antioxidants in kidney tissues

Nitric oxide (NO), malondialdehyde (MDA), superoxide dismutase (SOD), and catalase (CAT) were determined in the homogenate solution of kidney tissue (500 mg kidney tissue homogenized in certain buffer according to manufacturing instructions) colorimetrically using kits (Biodiagnostic, Egypt). The assay of NO relies on that the nitrate (NO₃) in the sample is converted to nitrite (NO₂) by the nitrate reductase enzyme. Next, total nitrite is detected with Griess Reagents as a colored azo dye product (absorbance 540 nm) (Miranda et al., 2001). MDA reacts with thiobarbituric acid (TBA) in acidic medium at temperature of 95 °C for 30 min to form thiobarbituric acid reactive product the absorbance of the resultant pink product can be measured at 534 nm (Koga et al., 2012). The assay

of SOD relies on the enzyme ability to inhibit the phenazine methosulphate-mediated reduction of nitroblue tetrazolium dye (Nishikimi et al., 1972). Catalase reacts with a known quantity of H_2O_2 . The reaction is stopped after exactly one minute with catalase inhibitor. In the presence of peroxidase (HRP), the remaining H_2O_2 reacts with 3,5-Dichloro-2-hydroxybenzene sulfonic acid (DHBS) and 4-aminoantipyrine (AAP) to form a chromophore with a color intensity inversely proportional to the amount of catalase in the original sample (Aebi, 1984).

2.9. Real-time PCR analysis

According to Khedr et al. (2022), Total RNA was isolated from kidney tissues using the Trizol reagent. To synthesis cDNA from 1 μ g RNA, a cDNA reverse transcription kit was utilized. SYBER Green PCR Master Mix was used for the RT-PCR investigation, which was carried out using an Applied Biosystem (Step One™, USA). $2^{-\Delta\Delta Ct}$ equation was used to estimate Caspase-3, TNF α , IL-6, TGF β -1, Bcl2, β -catenin, and fibronectin expression. Table 1 contains primers of genes.

2.10. Histopathological investigation

Half of the Kidney for each rat was immediately fixed in 10% buffered formalin. The fixed specimens were dehydrated in ascending grades of ethyl alcohol, cleared in xylene, and embedded in paraffin at 60 °C. Five μ m thicknesses of kidney were cut by microtome, deparaffinized with xylene, rehydrated by descending grades of ethanol concentration (100–95–75%) and stained routinely with haematoxylin and eosin for illustration of the histological studies. The specimens were investigated under a light microscope at 400x magnification (Banchroft et al., 1996).

2.11. Immunohistochemical examination of renal caspase-3 and β -catenin

Caspase-3 and β -catenin expression in the paraffin-embedded slices (3 μ m thickness) of kidney tissues was investigated to show the apoptosis and fibrosis in renal tissues according to Khedr et al. (2022) and examined with a light microscope at 400x magnification.

2.12. Statistical analysis

The statistical analysis of the results, including the mean, standard deviation, and p values, was performed using Statistical Package for Social Science (SPSS) version 22.0. Data were analyzed statistically using one-way analysis of variance (ANOVA) followed by posthoc multiple comparisons (Tukey test) at $p \leq 0.05$.

Table 1
PCR primers.

Gene	Accession no.	Primer sequences
TGF β -1	NM_021578.2	F: 5'-CACTCCCCTGGCTTCTAGTG-3' R: 5'-GGACTGGCGAGCCTTAGTTT-3'
IL-6	NM_012589.2	F: 5'-GCCCTTCAGGAACAGCTATGA-3' R: 5'-TGTCACAACATCAGTCCCAAGA-3'
β -Catenin	NM_053357.2	F: 5'-TGAAGGTGCTGTCTGTCTGCTC-3' R: 5'-TGCATCGGACAAGTTTCTCAGA-3'
Fibronectin	NM_082612.1	F: 5'-GTGGCTGCGCTTCAACTTCTC-3' R: 5'-GTGGGTTGCAAACTTCAAT-3'
Caspase-3	NM_012922.2	F: 5'-GGACCTGTGGACCTGAAAAA-3' R: 5'-GCATGCCATATCATCGTCAG-3'
Bcl2	NM_016993.1	F: 5'-GGTGAACCTGGGGAGGATTG-3' R: 5'-GCATGTGGGCCATATAGT-3'
GAPDH	NM_017008.4	F: 5'-AGACAGCCGCATCTTCTGT-3' R: 5'-TTCCATTCTCAGCCTTGAC-3'

3. Results

3.1. BMSCs isolation and culture

Mesenchymal stem cells were extracted from adipose tissues surrounding the rat testes by enzymatic method. The main isolated cells were spindle during the first five days of growth, though some were also spherical, flat, and fibroblast-like cells (Fig. 1A). Cultures contained a uniform monolayer of fibroblastic cells after the third passage (Fig. 1B).

3.2. Characterization of MSCs by flow cytometer

After passage 3, the cells were characterized by flow cytometry. CD34 was expressed negatively by MSCs (98.2%), while CD90 was expressed positively by MSCs (91.6%). These findings are compatible with BMSCs' immunophenotype (Fig. 2A, B).

3.3. Renal immunofluorescence with BrdU labeling

Mesenchymal stem cells stained with BrdU were placed in the kidney and distributed in glomeruli (Fig. 3).

3.4. Effect of dexpanthenol and MSCs on renal functions of rats injected with cisplatin

In comparison to the normal group, the cisplatin group exposed statistically significant increase in Cr, BUN, and MAU at 5 and 12 days. The dexpanthenol and MSCs treated group exerted a reno-protective effect more than each of them alone, as reflected by significantly decrease of SCr, BUN, and MAU at 5 and 12 days ($P < 0.05$) compared with the cisplatin group (Table 2).

3.5. Effect of dexpanthenol and MSCs on renal oxidative stress and antioxidants of rats injected with cisplatin

The cisplatin group represented an increase in renal NO and MDA levels and inhibition in SOD and CAT activities at the 5th and 12th days of rats' sacrifice compared to the values of the normal group at the same 2 time intervals. Conversely, the cisplatin & dexpanthenol & MSCs group revealed a decrease in NO and MDA levels and increase in CAT and SOD activities compared to the cisplatin group at the 5th and 12th days ($P < 0.05$) (Table 3).

3.6. Effect of dexpanthenol and MSCs on renal inflammatory genes (IL-6 and TGF β -1), apoptotic genes (Bcl2 and Caspase-3), and fibrotic genes (Fibronectin and β -catenin) of rats injected with cisplatin

The cisplatin group represented a significant increase in renal IL-6, TGF β -1, Caspase-3, Fibronectin, and β -catenin expression and down-regulation of Bcl2 at the 5th and 12th days of rats' sacrifice compared to the values of the normal healthy group at the same 2 time intervals. In contrast, the cisplatin & dexpanthenol & MSCs group revealed a significant inhibition in expression of IL-6, TGF β -1, Caspase-3, Fibronectin, and β -catenin and up-regulation of Bcl2 compared to the cisplatin group at 2 time intervals (5th and 12th days) ($P < 0.05$) (Fig. 4).

3.7. Histopathological investigation

A representative photomicrograph of the kidney from different treatments at 5 days post exposure is represented in (Fig. 5). Control kidney with normal histological appearance of renal tubules and glomerulus (Fig. 5A). Cisplatin group showing diffuse intraluminal eosinophilic, homogenous, proteinaceous fluid, inset tubular

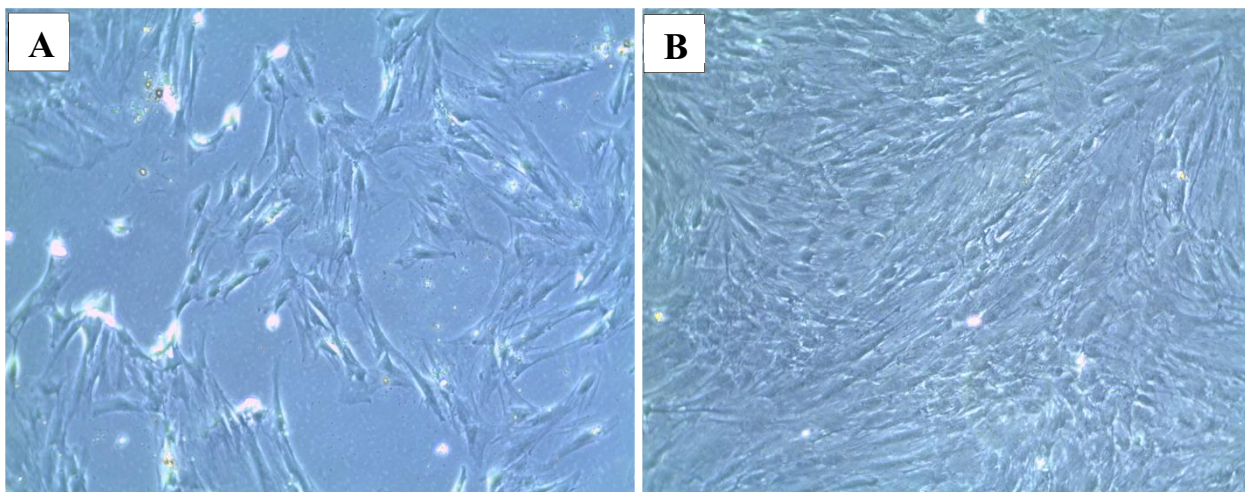


Fig. 1. a) Rounded MSCs after 5 days of culture, b) Spindle adherent cells at passage 3.

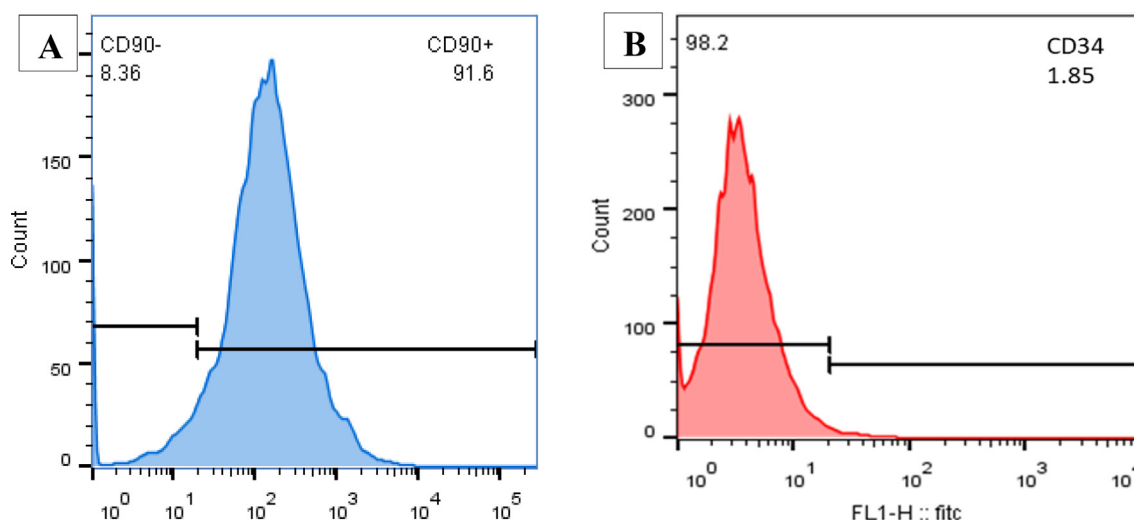


Fig. 2. Immunophenotypic analysis of mesenchymal stem cells disclosed their positive expression for CD90 (A) and negative expression for CD34 (B).

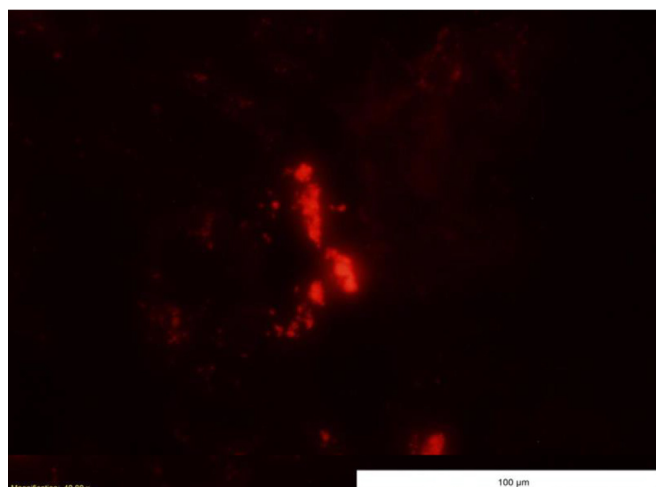


Fig. 3. Labeled MSCs with BrdU in renal tissue.

Table 2
Effect of dexpanthenol and MSCs on renal function.

	5 days	12 days
Creatinine (mg/dl)		
Control	0.37 ± 0.07	0.43 ± 0.09
Cis	5.2 ± 0.38 ^a	1.9 ± 0.24 ^a
Cis + Dexa	2.89 ± 0.28 ^{ab}	1.5 ± 0.08 ^{ab}
Cis + MSCs	1.97 ± 0.39 ^{ab}	0.98 ± 0.23 ^b
Cis + MSCs + Dexa	0.88 ± 0.3 ^b	0.6 ± 0.2 ^b
BUN (mg/dl)		
Control	19.97 ± 0.98	20.7 ± 0.7
Cis	96 ± 5.2 ^a	75.3 ± 4.9 ^a
Cis + Dexa	72.08 ± 3.34 ^{ab}	51.37 ± 1.29 ^{ab}
Cis + MSCs	49.01 ± 2.8 ^{ab}	32.9 ± 0.96 ^{ab}
Cis + MSCs + Dexa	36 ± 2.81 ^{ab}	29.04 ± 2.03 ^{ab}
MAU (mg/dl)		
Control	1.08 ± 0.32	0.89 ± 0.07
Cis	3.6 ± 0.23 ^a	1.98 ± 0.2 ^a
Cis + Dexa	1.67 ± 0.22 ^{ab}	1.49 ± 0.2 ^{ab}
Cis + MSCs	1.27 ± 0.21 ^b	1.17 ± 0.03 ^b
Cis + MSCs + Dexa	1.19 ± 0.24 ^b	0.96 ± 0.07 ^b

Significant difference compared to corresponding ^aControl and ^bCis groups by one-way analysis of variance (ANOVA) followed by posthoc multiple comparisons (Tukey test) at p ≤ 0.05.

Table 3
Effect of MSCs and dexpanthenol treatment on oxidative stress and antioxidants.

	5 days	12 days
MDA (nmol/g kidney tissue)		
Control	18.27 ± 2.05	20.37 ± 1.47
Cis	65.53 ± 6.42 ^a	59.06 ± 4.77 ^a
Cis + Dexa	57.58 ± 8.62 ^b	45.71 ± 4.91 ^{ab}
Cis + MSCs	54.25 ± 6.75 ^{ab}	42.37 ± 4.49 ^{ab}
Cis + MSCs + Dexa	42.58 ± 5.81 ^{abcd}	30.12 ± 3.23 ^{abcd}
NO (nmol/g kidney tissue)		
Control	9.76 ± 1.33	9.55 ± 0.81
Cis	58.96 ± 4.44 ^a	56.9 ± 2.86 ^a
Cis + Dexa	46.14 ± 6.25 ^{ab}	37.02 ± 8.82 ^{ab}
Cis + MSCs	42.81 ± 5.12 ^{ab}	32.02 ± 6.72 ^{ab}
Cis + MSCs + Dexa	37.21 ± 4.13 ^{ab}	24.89 ± 7.04 ^{abd}
SOD (U/g kidney tissues)		
Control	206.33 ± 13.9	201.17 ± 21.08
Cis	95.91 ± 18.76 ^a	110.5 ± 13.51 ^a
Cis + Dexa	120.33 ± 9.61 ^a	151.5 ± 16.04 ^{ab}
Cis + MSCs	128.66 ± 13.14 ^{ab}	156.5 ± 19.11 ^{ab}
Cis + MSCs + Dexa	153.9 ± 14.6 ^{ab}	177.5 ± 13.31 ^b
CAT (U/g kidney tissues)		
Control	5.19 ± 0.59	5.17 ± 0.42
Cis	1.33 ± 0.47 ^a	1.64 ± 0.24 ^a
Cis + Dexa	2.19 ± 0.4 ^a	3.13 ± 0.4 ^{ab}
Cis + MSCs	2.56 ± 0.52 ^{ab}	3.46 ± 0.46 ^{ab}
Cis + MSCs + Dexa	2.71 ± 0.73 ^{ab}	4.2 ± 0.49 ^b

Significant difference compared to corresponding ^aControl, ^bCis, ^cDexa, and ^dMSCs group by one-way analysis of variance (ANOVA) followed by posthoc multiple comparisons (Tukey test) at $p \leq 0.05$.

epithelium showing necrosis and vacuolation, and regenerative epithelium with a large vesiculate nucleus in addition to the luminal hyaline cast, H&E, 400x (Fig. 5B). Cisplatin exposed group showing numerous cortical tubules showing diffuse epithelial sloughing with ectatic tubules, epithelial vacuolation also detected, and mildly undulant capsule, Inset, higher magnification on different tubular epithelial changes (degenerative vacuolation, sloughing in addition to atrophied tubules), H&E, 400x (Fig. 5C). Cisplatin & dexpanthenol exposed group showing restoration of normal renal architectures of tubules and glomerulus, inset, regenerative features characterized by tubular basophilic cytoplasm, large vesiculate nuclei with a prominent nucleolus, H&E, 400x (Fig. 5D). Cisplatin & Stem cells exposed group showing up to 80% of tissue had normal tubular and glomerular architecture with mild, focal interstitial nephritis and minimal, occasional luminal cast and few tubular necrosis and hypertrophied parietal cells of glomerulus, H&E, 100x, inset, lymphoplasmatic interstitial aggregations with enlarged tubular epithelial cell nuclei up to 2–3 times normal size with marginated chromatin (regenerative features), H&E, 400x (Fig. 5E). Cisplatin & Stem cells & dexpanthenol exposed group showed few renal casts, few tubules with attenuated epithelium and moderate tubulorrhexis and vacuolation in addition to occasional, focal, minimal glomerular changes with mild dilatation of the uriniferous spaces, H&E, 100x inset, section showing most tubules with normal tubular epithelial architecture and few, minimal intraluminal sloughed tissue, H&E, 400x (Fig. 5F).

A representative photomicrograph of the kidney from different treatments at 12 days post exposure is represented in (Fig. 6). Cisplatin group showed up to 70% of tubules are dilated ectatic with few intraluminal hyaline cast and occasional deeply basophilic intraluminal granular mineral, inset, tubules are dilated and lined with attenuated epithelium, H&E, 400x (Fig. 6A). Diffusely, tubular epithelium shows necrosis characterized by loss of cellular detail, indistinct cell borders, hyper eosinophilic cytoplasm, nuclear karyolysis, pyknosis, and epithelial detachment from intact basement membranes with multifocal glomerular damage, inset, mesangiolysis with pyknotic or karyorrhectic endothelial or mesangial nuclei and dilated uriniferous spaces with irregularity in parietal epithe-

lial lining, H&E, 400x (Fig. 6B). Cisplatin group showed interstitial nephritis characterized by focal tubular damage infiltrated with numerous lymphocytes, plasma cells admixed with fibroblasts (fibrosis), H&E, 400x (Fig. 6C). Diffuse detached tubular epithelium with variable amount of intraluminal deeply basophilic granular materials (mineral), few tubules showed hyaline cast, H&E, 100x, inset, complete loss of tubular architecture with either complete loss of nucleus or large vesiculate nucleus with marginated chromatin beside the deeply basophilic minerals, H&E, 400x (Fig. 6D). Cisplatin & dexpanthenol group showed restoration of up to 90% of tubular and glomerular architecture with occasional tubular necrosis and intraluminal cellular cast, H&E, 100x, inset showed the regeneration of most renal architecture, some tubules piled up with a moderate amount of amphophilic cytoplasm and large round, more densely basophilic nuclei in addition to few, individual tubular damage, H&E, 400x (Fig. 6E). Cisplatin & stem cells showed regeneration of most renal tissue architecture with minimal tubular vacuolation and occasional luminal cast, Inset showed restored glomerular and tubular architecture and individual vacuolated cells, H&E, 400x (Fig. 6F). Cisplatin & stem cells & dexpanthenol showed restoration of renal architecture with high regenerative features, Inset, individual tubular cell pyknosis with hypertrophied epithelial cells which pile up, have more basophilic cytoplasm, vesiculate nuclei with prominent nucleoli, and rare mitotic figures (Fig. 6G).

3.8. Immunohistochemical examination

3.8.1. Apoptotic marker Caspase-3

Caspase-3 immunohistochemical staining of kidney sections of rats at 5 and 12 days post exposure to different treatments is represented in (Fig. 7). Kidney sections of normal rats (Fig. 7A). B-E indicate caspase-3 expression at 5 days post exposure, F-I indicate expression at 12 days post exposure. Cisplatin group showed diffuse intensely stained immune positivity (Fig. 7B). Groups treated with cisplatin & dexpanthenol showed diffuse, intraluminal, moderate number of immunopositive staining (Fig. 7C), while group treated with cisplatin & MSCs showing decreased numbers of immune-reactive cells with faint tubular cytoplasmic immunopositivity (Fig. 7D). Interestingly, combination group diffuse faint tubular immunopositivity (Fig. 7E). At 12 days post exposure, the expression was still diffuse and strong in cisplatin exposed group (Fig. 7F). Meanwhile, the expression in the other groups decreased slightly with the treatment with dexpanthenol and MSCs alone (Fig. 7G, 7H), notably, the group treated with both dexpanthenol and MSCs showed a greater decrease in caspase-3 expression (Fig. 7I). Arrows indicated positivity expression, the original image at 100x and the boxed one at 400x.

3.8.2. Fibrotic marker β -catenin

β -catenin immunohistochemical staining of kidney sections of rats at 5 and 12 days post exposure to different treatments is presented in (Fig. 8). Diffuse strong β -catenin immunostained in renal tubules was observed in the cisplatin exposed group (Fig. 8B). In renal tubules, the location of β -catenin in the cytoplasm, nucleus, and lumina was clearly visible. Intraluminal positive immunostaining was seen inside the ectatic tubules of the cisplatin & dexpanthenol exposed group (Fig. 8C). Mild, multifocal faint tubular cytoplasmic positivity in cisplatin & stem cells (Fig. 8D). Diffuse faint tubular immunostaining was detected in the combination group (Fig. 8E). The expression of β -catenin at 12 days in different treatments was decreased compared with 5 days (Fig. 8F-I). Arrows indicated positivity expression, the original image at 100x and the boxed one at 400x.

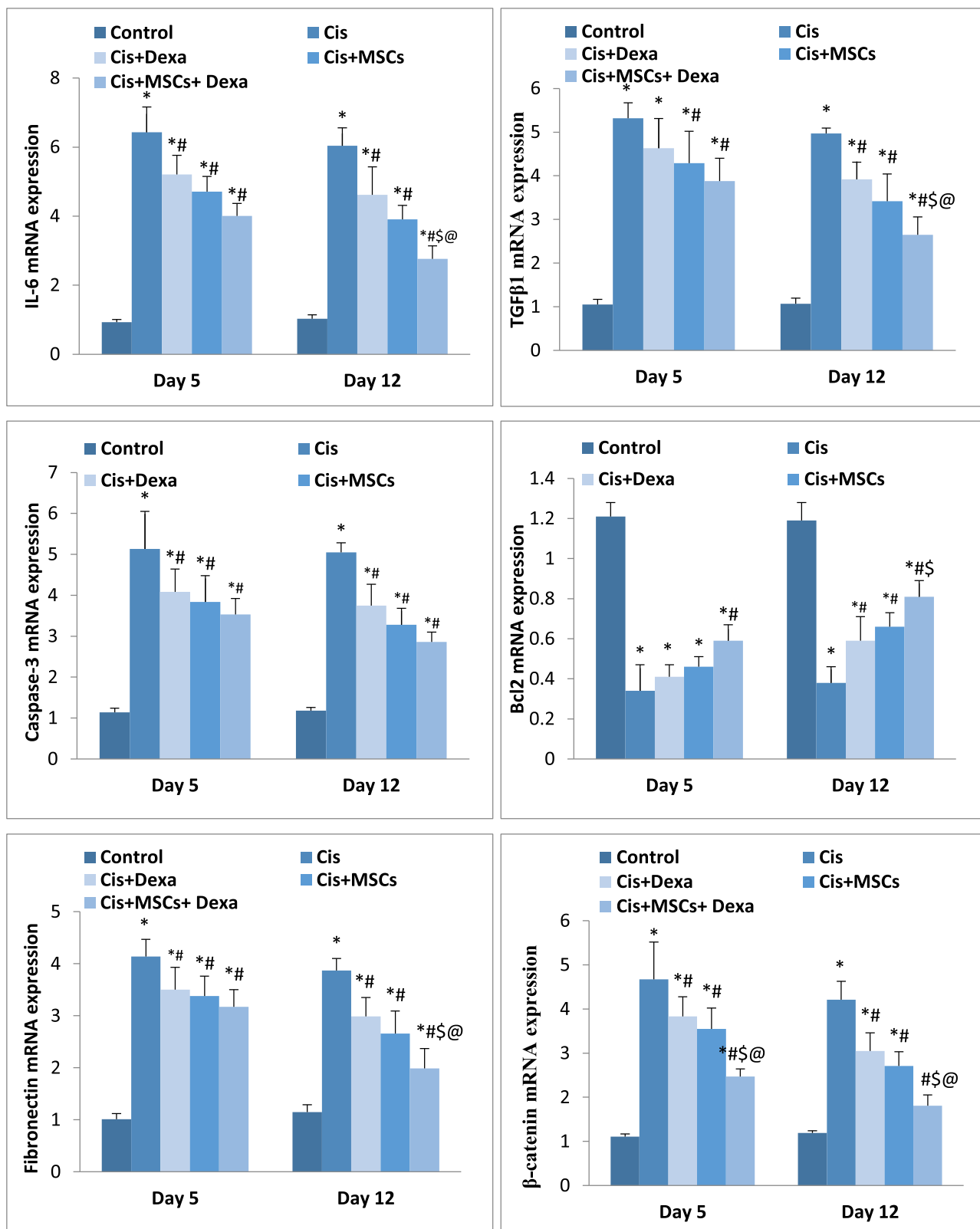


Fig. 4. Effect of Dexpanthenol and MSCs on renal inflammatory genes (IL-6 and TGFβ-1), apoptotic genes (Caspase-3 and Bcl2), and fibrotic genes (Fibronectin and β-catenin) of rats injected with cisplatin. Significant difference compared to corresponding *Control, #Cis, \$Dexa, and @MSCs group by one-way analysis of variance (ANOVA) followed by post hoc multiple comparisons (Tukey test) at $p \leq 0.05$.

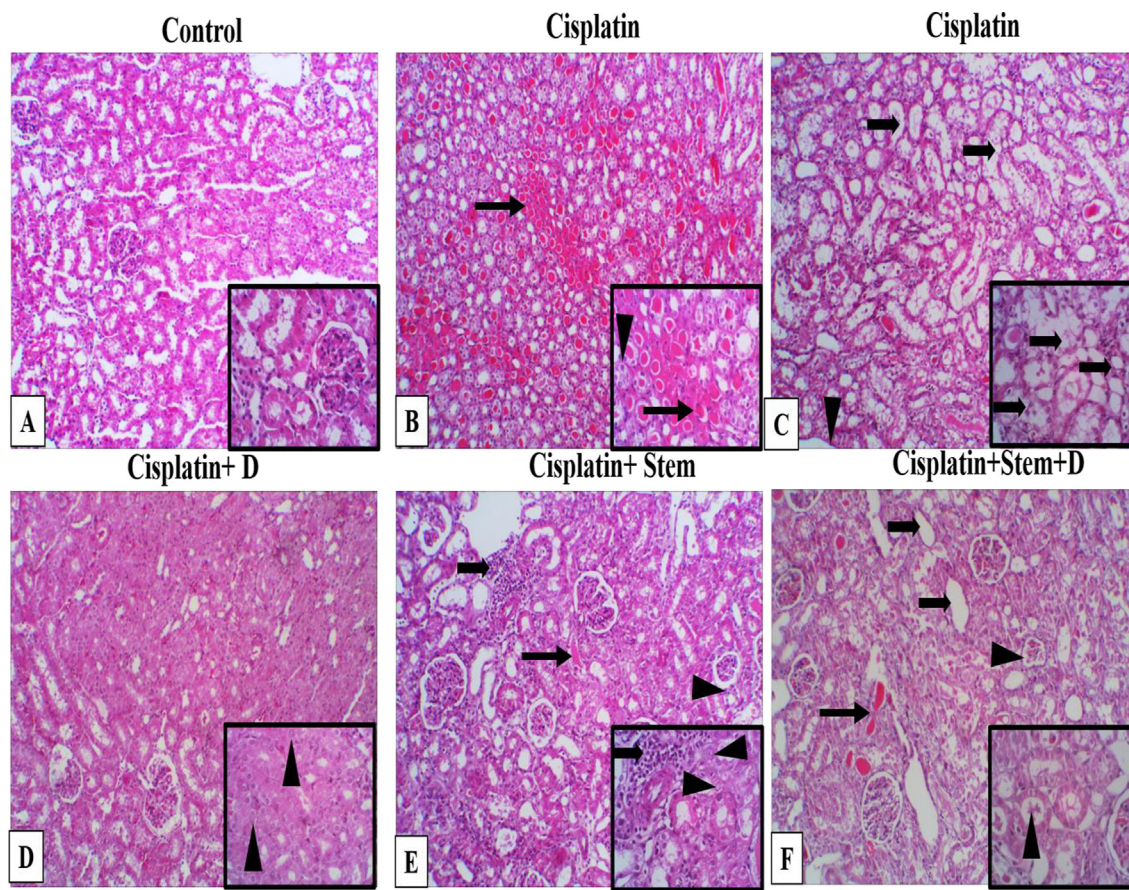


Fig. 5. Photomicrographs of H&E stained renal sections in rats euthanized after 5 days in control group (A), cisplatin group (B, C) showing diffuse intraluminal eosinophilic, homogenous, proteinaceous fluid admixed with sloughed tubular epithelial cells and necrotic debris (granular casts) (thin arrow), inset tubular epithelium showing necrosis and vacuolation and regenerative epithelium with large vesiculate nucleus (arrow head) in addition to the luminal hyaline cast (thin arrow), C) showing numerous cortical tubules showing diffuse epithelial sloughing with ectatic tubules (thick arrow), epithelial vacuolation also detected and mildly undulant capsule (arrow head), inset, higher magnification on different tubular epithelial changes (degenerative vacuolation, sloughing in addition to atrophied tubules) (thick arrows). Cisplatin group treated with dexpanthenol (D) showing restoration of normal renal architectures of tubules and glomerulus, inset, regenerative features characterized by tubular basophilic cytoplasm, large vesiculate nuclei with a prominent nucleolus (arrow head). Cisplatin group treated with stem cells (E) showing up to 80% of tissue had normal tubular and glomerular architecture with mild, focal interstitial nephritis (thick arrow) and minimal, occasional luminal cast (thin arrow) and few tubular necrosis and hypertrophied parietal cells of glomerulus (arrow head) inset, lymphoplasmatic interstitial aggregations (thick arrow) with enlarged tubular epithelial cell nuclei up to 2–3 times normal size with margined chromatin (regenerative features) (arrow head) and group treated with dexpanthenol and stem cells (F) showing few renal cast (thin arrow), few tubules with attenuated epithelium (thick arrows) and moderate tubulorrhexis and vacuolation in addition to occasional, focal, minimal glomerular changes with mild dilatation of the uriniferous spaces (arrow head) inset, section showing most tubules with normal tubular epithelial architecture and few, minimal intraluminal sloughed tissue (arrow head), the original image at 100x and the boxed one at 400x.

4. Discussion

In the current study, MSCs were isolated from adipose tissues surrounding the male rat testes by enzymatic method. Then these cells were cultured with DMEM. This isolation method is in agreement with (Salehinejad et al., 2012) who confirmed that, the isolation of MSCs by using an enzymatic method is an excellent and the most rapid method to isolate MSCs within 24–48 hr. In our study, flow cytometry analysis of the cultured cells revealed that they were positive for CD90, with 91.9% and negative for CD34, with 1.85%. This is in agreement with (Salehinejad et al., 2012). Similarly, other investigations supported the finding that ADMSCs displayed significant positivity for MSC markers such as CD73, CD105, and CD90, as well as integrin markers such as CD44 and CD29, but were negative for an endothelial cell marker such as CD31 or hematopoietic cell indicators such as CD45 (Zhang et al., 2012). The worldwide organization for cellular treatment has identified several proven characteristics of MSCs, including plastic adherence, a particular collection of cell surface markers (CD73, CD90, and CD105), and the lack of CD14, CD34, and CD45 (Bai et al., 2016).

These criteria were met by the separated cells, indicating that they are MSCs.

The present findings revealed that cisplatin dose induced nephrotoxicity and resulted in a significant increase in markers of renal function in the cisplatin group compared to normal after 5 and 12 days from cisplatin injection. According to Perše and Večerić-Haler, (2018), increased nephrotoxicity markers, like BUN and creatinine, are typically noticed 3–7 days after intraperitoneal administration and then return to baseline levels after 14 days when a single high nephrotoxic dose of cisplatin is used (for example, 5–10 mg/kg in rats). Seven days following the cisplatin injection, the first indications of structural regeneration were seen. Urinary albumin excretion is used to detect tubular dysfunction induced by cisplatin, so elevated microalbuminuria concentration is indicative of high permeability of albumin in glomerulus (Charlton et al., 2014). This nephrotoxicity of cisplatin after 7 days from injection was confirmed by histopathological examination. Similar findings were reported previously by Barakat et al. (2020). The current study exposed that dexpanthenol attenuated the nephrotoxicity of cisplatin. This was evidenced by the

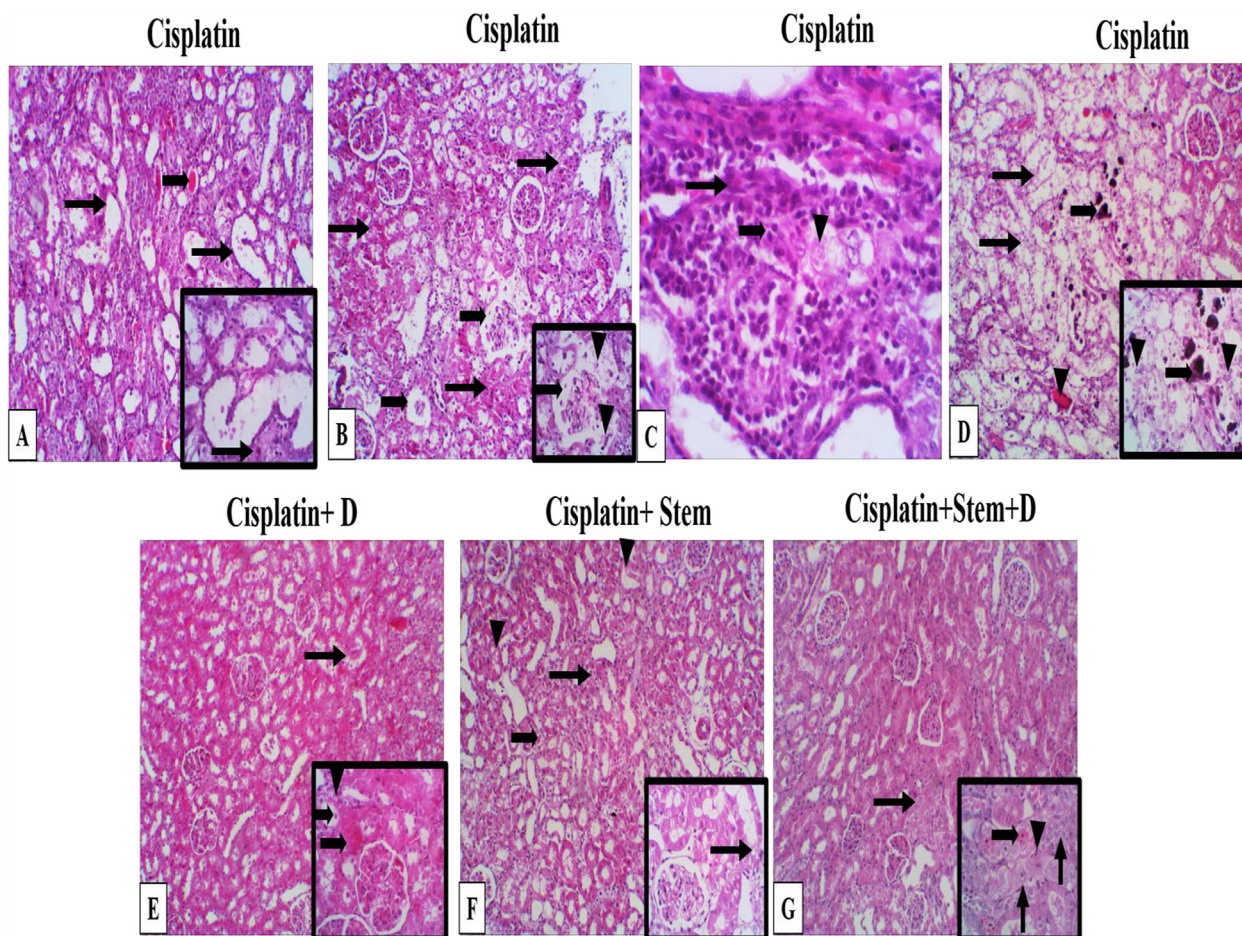


Fig. 6. Photomicrographs of H&E stained renal sections in rats euthanized after 12 days in control group (A), cisplatin group (A-D), A) showing up to 70% of tubules are dilated ectatic (thin arrows) with few intraluminal hyaline cast (thick arrow) and occasional deeply basophilic intraluminal granular mineral, inset, tubules are dilated and lined with attenuated epithelium. B) Diffusely, tubular epithelium shows necrosis characterized by loss of cellular detail, indistinct cell borders, hyper eosinophilic cytoplasm, nuclear karyolysis, pyknosis and epithelial detachment from intact basement membranes (thin arrows) with multifocal glomerular damage (thick arrows), inset, mesangiolysis with pyknotic or karyorrhectic endothelial or mesangial nuclei (arrow head) and dilated uriniferous spaces (thick arrow) with irregularity in parietal epithelial lining. C) Showing interstitial nephritis characterized by focal tubular damage (arrow head) infiltrated with numerous lymphocytes (thick arrow), plasma cells admixed with fibroblasts (fibrosis) (thin arrow). D) Diffuse detached tubular epithelium (thin arrow) with variable amount of intraluminal deeply basophilic granular materials (mineral) (thick arrow), few tubules showed hyaline cast (arrow head) inset, complete loss of tubular architecture with either complete loss of nucleus or large vesiculate nucleus with margined chromatin (arrow heads) beside the deeply basophilic minerals (thick arrow). Cisplatin group treated with dexpanthenol (E) showing restoration of up to 90% of tubular and glomerular architecture with occasional tubular necrosis and intraluminal cellular cast (thin arrow) inset showing the regeneration of most renal architecture, some tubules piled up with a moderate amount of amphophilic cytoplasm and large round, more densely basophilic nuclei (arrow head) in addition to few, individual tubular damage (thick arrows). Cisplatin group treated with stem cells (F) showing regeneration of most renal tissue architecture with minimal tubular vacuolation (thin arrow) and occasional luminal cast (thick arrow), Inset showing restored glomerular and tubular architecture and individual vacuolated cells (thin arrow). Group treated with dexpanthenol and stem cells (G) showing restoration of renal architecture with high regenerative features (thin arrow), inset, individual tubular cell pyknosis (thick arrow) with hypertrophied epithelial cells which pile up, have more basophilic cytoplasm, vesiculate nuclei with prominent nucleoli (thin arrows), and rare mitotic figures (arrow head), the original image at 100x and the boxed one at 400x.

inhibition in BUN, creatinine, and microalbuminuria in dexpanthenol & cisplatin group compared to cisplatin group after 5 and 12 days of injection. These findings are in the same line with Bilgic et al. (2018), who stated that dexpanthenol could enhance renal function through reduction of creatinine, BUN, and microalbuminuria levels in cisplatin-preserved animals compared to cisplatin group. Moreover, histological findings showed that the co-administration of dexpanthenol significantly improved the histopathological changes of cisplatin by increasing regenerative changes in dexpanthenol and cisplatin group at 5th and 12th days, with more regenerative changes after 12 days. This finding is in agreement with Pinar et al. (2022). Also, results of this study revealed that MSCs decreased nephrotoxicity of cisplatin. This result is in harmony with Liu et al. (2020), who suggested that ADMSCs released biologically active factors to treat the injured kidney, as they prevented the toxicity of cisplatin in renal proximal tubular cells. Histopathological changes showed that MSCs and cis-

platin treated group at the 5th day showed 80% of normal tubular and glomerular architecture. On the 12th day, there was a regeneration of most renal tissue architecture. This is compatible with Yao et al. (2015) who stated the same histopathological observations. Interestingly, group treated with both dexpanthenol and MSCs after cisplatin injection revealed the most decrease in the creatinine, BUN, and microalbuminuria and the most improvement in the kidney structure, suggesting the impact of both on nephrotoxicity. Histopathological investigation of this group showed restoration of renal architecture with high regenerative features.

In the present study, NO and MDA levels increased and CAT and SOD levels decreased in cisplatin group at 5th and 12th days. By suppressing antioxidant enzymes and elevating ROS, cisplatin disrupts the body's natural antioxidant protection. It also promotes the release of lipid peroxidation, in which free radicals target the polyunsaturated fatty acids in cell membranes, and an increased breakdown of cells and renal tissues. The resultant nephrotoxicity

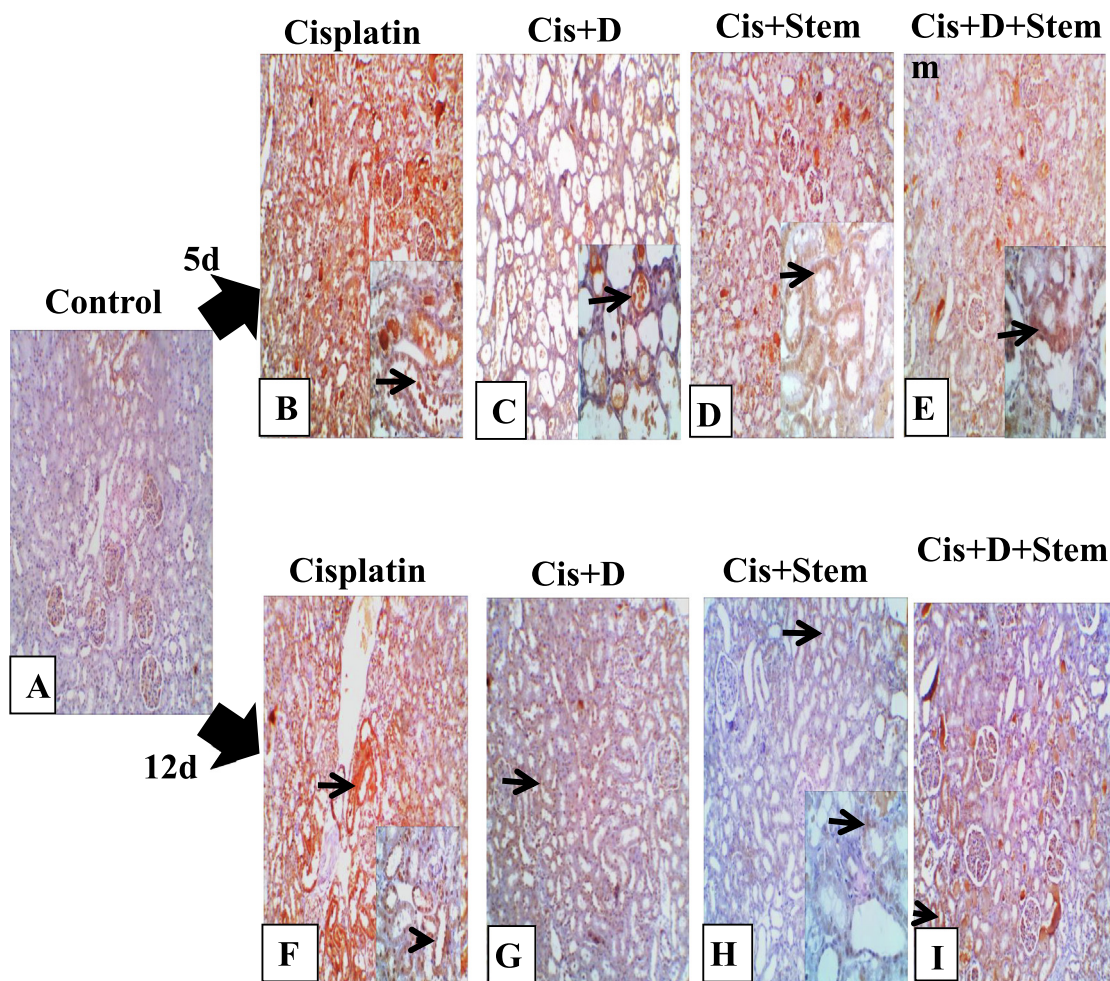


Fig. 7. Photomicrographs of immunostained renal sections against Caspase-3 of rats sacrificed after 5 and 12 days in control group (A), cisplatin group (B, F), cisplatin groups treated with dexpanthenol (C, G) or stem cells (D, H) and group treated with dexpanthenol and stem cells (E, I). Arrow indicate positivity, the original image at 100x and the boxed one at 400x.

is the outcome of this elevated oxidative stress, which damages DNA (Fang et al., 2021). The present study clarified that in kidney tissues, (MDA and NO) were decreased and (SOD and CAT) levels were increased in dexpanthenol and cisplatin treated group compared to group of cisplatin at 5th and 12th days of rats' sacrifice. Turgut et al. (2013) stated that dexpanthenol is an antioxidant. Furthermore, dexpanthenol increased antioxidants (CAT and SOD) and reduced oxidative stress (NO and MDA) in kidney tissues. In addition, this study induced that in the kidney tissue, MDA and NO were significantly reduced, however CAT and SOD were improved in MSCs and cisplatin treated group compared to group of the cisplatin at 5th and 12th days of rats' sacrifice. This could be explained by Chi et al. (2019), who stated that the ability to effectively remove peroxides and nitrous peroxide anions was maintained by MSCs by providing constant production of SOD, glutathione peroxidase 1, and CAT. Through the suppression of MDA and NO, MSCs can also detoxify toxic substances and reduce the risk of oxidative damage. Consequently, administration of dexpanthenol and MSCs could remodeling the antioxidant defense system by reducing free radicals (NO and MDA) and induce antioxidant enzymes (SOD and CAT).

In addition, IL-6 and TGF- β 1 were increased in rats injected with cisplatin after 5 and 12 days, respectively. This result is consistent with previous studies that demonstrated that cisplatin increases the fibrogenic cytokines (TGF- β 1 and IL-6), that stimulate

production of extracellular matrix proteins and cause fibrosis of kidney (Bayomi et al., 2013; Humanes et al., 2017; Leo et al., 2021). The present study revealed that treatment with dexpanthenol and/or MSCs after cisplatin injection represents inhibition in IL-6 and TGF- β 1 levels in kidney tissue when compared with group of cisplatin at the 5th and 12th days of rats' sacrifice. Hassaan et al. (2021) revealed that dexpanthenol down-regulates IL-6 and TGF- β 1. Moreover, Adnan et al. (2020) have stated that the use of dexpanthenol decreased IL-6, TNF- α , and IL-1 β levels, and IL-6 synthesis. MSCs suppress B cells from producing autoantibodies as well as T helper and effector T cells. TGF- β and IL-6 are potent pro-inflammatory cytokines. A prior study revealed that MSCs might impede Th1 and Th2 differentiation and simultaneously suppress IL-6 and TGF- β (Darlan et al., 2020).

This study reported an up-regulation of caspase-3 and correlated that with the down-regulation of Bcl2 in the kidney tissue at the 5th and 12th days of cisplatin injection. A similar result was exposed in an immunohistochemical examination of caspase-3. According to Neamatallah et al. (2018), cisplatin stimulated the expression of BAX and caspase-3 while decreasing Bcl2 expression due to stimulation of caspase-3 that causes apoptosis. In contrast, Bcl-2 was up-regulated and caspase-3 was down-regulated in the kidney tissue after treating the experimental rats with dexpanthenol and/or MSCs after cisplatin injection. This came in line with an immunohistochemical examination of caspase-3.

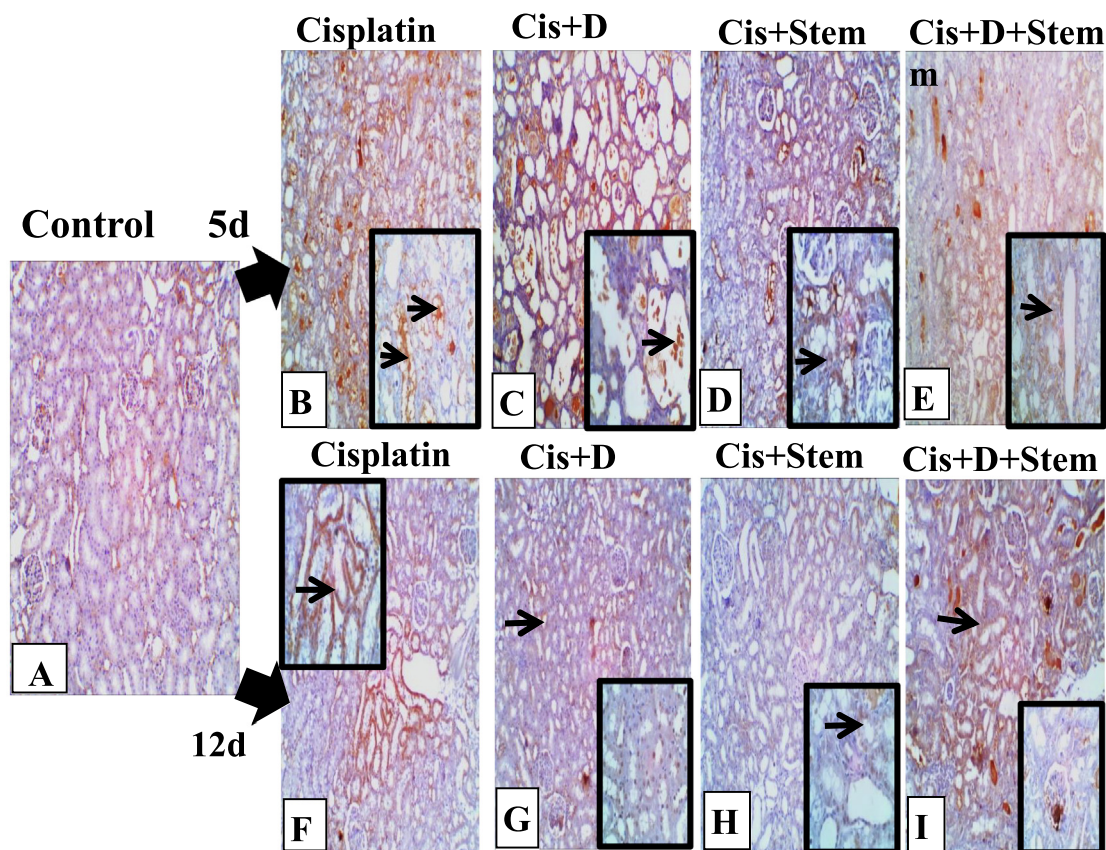


Fig. 8. Photomicrographs of immunostained renal sections against β -catenin of rats sacrificed after 5 and 12 days in control group (A), cisplatin group (B, F), cisplatin groups treated with dexpanthenol (C, G) or stem cells (D, H) and group treated with dexpanthenol and stem cells (E, I). Arrow indicate positivity, the original image at 100x and the boxed one at 400x.

Bilgic et al. (2018) showed that dexpanthenol decreased caspases and increased Bcl2 after cisplatin injection. Hua et al. (2015) exposed that Treatment with MSCs resulted in an increase in the Bcl2/Bax ratio as well as the up-regulation of Bcl2 and the down-regulation of Bax and caspase-3. Bcl2 prevents cytochrome C from being released from the mitochondria, which reduces apoptosis. Moreover, our study demonstrated that administration of both MSCs with dexpanthenol could have a more significant impact in reducing apoptosis than using each one alone.

As a result of the inflammation detected with the cisplatin injection, fibrosis was observed in the kidney tissues. The Wnt/ β -catenin signaling pathway is activated in AKI (Sun et al., 2020). In addition, Fibronectin increased due to cisplatin, that causes kidney fibrosis (Gao et al., 2016). β -catenin and Fibronectin expression was down-regulated in the kidney tissue by treatment of experimental rats with dexpanthenol and/or MSCs after cisplatin injection at 5th and 12th days of rats' sacrifice. This was in agreement with the protein expression of β -catenin observed with the immunohistochemical study. The role of dexpanthenol in decreasing β -catenin and fibronectin expression in kidney tissue was previously mentioned by Hassaan et al. (2021). MSCs are more regenerative and have anti-fibrotic and anti-inflammatory properties. MSCs reduced fibrosis, the expression of genes associated with fibrosis, such as β -catenin and fibronectin in rats (Ibrahim et al., 2021; Yoon et al., 2015). According to impact of dexpanthenol and MSCs on reducing fibrotic markers; β -catenin and Fibronectin in kidney tissue, it is logical to find that administration of them together could manifest a greater reduction in fibrosis caused by cisplatin as well as the reduction in inflammation, ROS, and improving kidney functions and architecture.

5. Conclusion

Dexpanthenol improved the ability of MSCs to protect against kidney damage. This improvement was supported by a reduction in the inflammation, fibrosis, and apoptosis induced by cisplatin, as well as an increase in antioxidants. Dexpanthenol with MSCs therapy may therefore be crucial for the creation of useful therapies.

6. Institutional review board statement

The Institutional Review Board (IRB) of the Faculty of Medicine at Mansoura University in Egypt gave its approval to the animal study protocol (MDP.22.09.109).

Declaration of Competing Interest

The authors declare that they have no known competing financial interests or personal relationships that could have appeared to influence the work reported in this paper.

Acknowledgments

Dr. Heba M. Adly and Dr. Saleh A.K. Saleh extend their appreciation to the Deputyship for Research & Innovation, Ministry of Education in Saudi Arabia for funding their work through the project number: IFP22UQU4240001DSR010.

References

- Aebi, H., 1984. Catalase in vitro. *Methods Enzymol.* 105, 121–126. [https://doi.org/10.1016/s0076-6879\(84\)05016-3](https://doi.org/10.1016/s0076-6879(84)05016-3).
- Alajez, N., Al-Ali, D., Vishnubalaji, R., Manikandan, M., Alfayez, M., Kassem, M., Aldahmash, A., 2018. Which stem cells to choose for regenerative medicine application: Bone marrow and adipose tissue stromal stem cells & #8211; Similarities and differences. *J. Nat. Sci. Med.* 1, 48–54. https://doi.org/10.4103/JNSM.JNSM_18_18.
- Azandeh, S., Orazizadeh, M., Hashemitabar, M., Khodadadi, A., Shayesteh, A.A., Nejad, D.B., Gharravi, A.M., Allahbakhshi, E., 2012. Mixed enzymatic-explant protocol for isolation of mesenchymal stem cells from Wharton's jelly and encapsulation in 3D culture system. *J. Biomed. Sci. Eng.* 5, 580–586.
- Bai, L., Li, D., Li, J., Luo, Z., Yu, S., Cao, S., Shen, L., Zuo, Z., Ma, X., 2016. Bioactive molecules derived from umbilical cord mesenchymal stem cells. *Acta Histochem.* 118, 761–769. <https://doi.org/10.1016/j.acthis.2016.09.006>.
- Banchroft, J. D., Stevens, A. and Turner, D.R., 1996. *Theory and practice of histological techniques*, Fourth Ed. Churchill Livingstone, New York, London, San Francisco, Tokyo. <https://doi.org/10.1136/jcp.36.5.609-d>.
- Barakat, L.A.A., Barakat, N., Zakaria, M.M., Khirallah, S.M., 2020. Protective role of zinc oxide nanoparticles in kidney injury induced by cisplatin in rats. *Life Sci.* <https://doi.org/10.1016/j.lfs.2020.118503>.
- Barakat, N., Barakat, L.A.A., Zakaria, M.M., Khirallah, S.M., 2021. Diacerein ameliorates kidney injury induced by cisplatin in rats by activation of Nrf2/Ho-1 pathway and Bax down-regulation. *Saudi J. Biol. Sci.* 28, 7219–7226. <https://doi.org/10.1016/j.sjbs.2021.08.025>.
- Bayomi, H.S., Elsherbiny, N.M., El-Gayar, A.M., Al-Gayyar, M.M.H., 2013. Evaluation of renal protective effects of inhibiting TGF- β type I receptor in a cisplatin-induced nephrotoxicity model. *Eur. Cytokine Netw.* 24, 139–147. <https://doi.org/10.1684/ecn.2014.0344>.
- Bilgic, Y., Akbulut, S., Aksungur, Z., Erdemli, M.E., Ozhan, O., Parlakpınar, H., Vardi, N., Turkoz, Y., 2018. Protective effect of dexpanthenol against cisplatin-induced hepatotoxicity. *Exp. Ther. Med.* 16, 4049–4057. <https://doi.org/10.3892/etm.2018.6683>.
- Cambiaso, C.L., Collet-Cassart, D., Lievens, M., 1988. Immunoassay of low concentrations of albumin in urine by latex particle counting. *Clin. Chem.* 34, 416–418.
- Charlton, J.R., Portilla, D., Okusa, M.D., 2014. A basic science view of acute kidney injury biomarkers. *Nephrol. Dial. Transplant.* 29, 1301–1311. <https://doi.org/10.1093/ndt/gft510>.
- Chi, H., Guan, Y., Li, F., Chen, Z., 2019. The effect of human umbilical cord mesenchymal stromal cells in protection of dopaminergic neurons from apoptosis by reducing oxidative stress in the early stage of a 6-OHDA-induced Parkinson's disease model. *Cell Transplant.* 28, 87–99. <https://doi.org/10.1177/0963689719891134>.
- Darlan D. M., D., Munir, D., Karmila Jusuf, N., Putra, A., Ikhsan, R., Alif, I., 2020. In vitro regulation of IL-6 and TGF- β by mesenchymal stem cells in systemic lupus erythematosus patients. *Med. Glas. (Zenica).* 17, 408–413. <https://doi.org/10.17392/1186-20>.
- Fang, C.-Y., Lou, D.-Y., Zhou, L.-Q., Wang, J.-C., Yang, B., He, Q.-J., Wang, J.-J., Weng, Q.-J., 2021. Natural products: potential treatments for cisplatin-induced nephrotoxicity. *Acta Pharmacol. Sin.* 42, 1951–1969. <https://doi.org/10.1038/s41401-021-00620-9>.
- Gao, W., Liu, Y., Qin, R., Liu, D., Feng, Q., 2016. Silence of fibronectin 1 increases cisplatin sensitivity of non-small cell lung cancer cell line. *Biochem. Biophys. Res. Commun.* 476, 35–41. <https://doi.org/10.1016/j.bbrc.2016.05.081>.
- Ghosh, S., 2019. Cisplatin: The first metal based anticancer drug. *Bioorg. Chem.* 88. <https://doi.org/10.1016/j.bioorg.2019.102925>.
- Hassaan, M., Elkashef, A., Barakat, N., Awadalla, A., Hashem, A., Soltan, M., Fathy El-Seddawy, M.-A.-M., 2021. Modulating effect of intraurethral dexpanthenol on urethral healing posturethroplasty: An experimental study in rats. *J. Urol.* 206, 2021.
- Hua, P., Liu, J., Tao, J., Liu, J., Yang, S., 2015. Influence of caspase-3 silencing on the proliferation and apoptosis of rat bone marrow mesenchymal stem cells under hypoxia. *Int. J. Clin. Exp. Med.* 8, 1624–1633.
- Humanes, B., Camaño, S., Lara, J.M., Sabbisetti, V., González-Nicolás, M.A., Bonventre, J.V., Tejedor, A., Lázaro, A., 2017. Cisplatin-induced renal inflammation is ameliorated by cilastatin nephroprotection. *Nephrol. Dial. Transplant. Off. Publ. Eur. Dial. Transpl. Assoc. - Eur. Ren. Assoc.* 32, 1645–1655. <https://doi.org/10.1093/ndt/gfx005>.
- Ibrahim, S., Fayed, A., Maher, A., 2021. Mesenchymal Stromal Cells Suppress Hepatic Fibrosis Via Modulating the Expression of Fibronectin and Integrin and Inhibiting DNA Fragmentation in Rats. *Arch. Med. Sci.* <https://doi.org/10.5114/aoms/134826>.
- Khedr, M., Barakat, N., El-deen, I.M., Zahran, F., 2022. Impact of preconditioning stem cells with all-trans retinoic acid signaling pathway on cisplatin-induced nephrotoxicity by down-regulation of TGF β 1, IL-6, and caspase-3 and up-regulation of HIF1 α and. *Saudi J. Biol. Sci.* 29, 831–839. <https://doi.org/10.1016/j.sjbs.2021.10.024>.
- Koga, H., Hagiwara, S., Kusaka, J., Goto, K., Uchino, T., Shingu, C., Kai, S., Noguchi, T., 2012. New α -lipoic acid derivative, DHL-HisZn, ameliorates renal ischemia-reperfusion injury in rats. *J. Surg. Res.* 174, 352–358. <https://doi.org/10.1016/j.jss.2011.01.011>.
- Leo, M., Schmitt, L.-I., Kutritz, A., Kleinschnitz, C., Hagenacker, T., 2021. Cisplatin-induced activation and functional modulation of satellite glial cells lead to cytokine-mediated modulation of sensory neuron excitability. *Exp. Neurol.* 341. <https://doi.org/10.1016/j.expneurol.2021.113695> 113695.
- Liu, D., Cheng, F., Pan, S., Liu, Z., 2020. Stem cells: a potential treatment option for kidney diseases. *Stem Cell Res. Ther.* 11, 249. <https://doi.org/10.1186/s13287-020-01751-2>.
- Luo, L., Guo, K., Fan, W., Lu, Y., Chen, L., Wang, Y., Shao, Y., Wu, G., Xu, J., Lü, L., 2017. Niche astrocytes promote the survival, proliferation and neuronal differentiation of co-transplanted neural stem cells following ischemic stroke in rats. *Exp. Ther. Med.* 13, 645–650. <https://doi.org/10.3892/etm.2016.4016>.
- Miranda, K.M., Espey, M.G., Wink, D.A., 2001. A rapid, simple spectrophotometric method for simultaneous detection of nitrate and nitrite. *Nitric Oxide* 5, 62–71. <https://doi.org/10.1006/niox.2000.0319>.
- Neamatallah, T., El-Shitany, N.A., Abbas, A.T., Ali, S.S., Eid, B.G., 2018. Honey protects against cisplatin-induced hepatic and renal toxicity through inhibition of NF- κ B-mediated COX-2 expression and the oxidative stress dependent BAX/Bcl-2/caspase-3 apoptotic pathway. *Food Funct.* 9, 3743–3754.
- Nishikimi, M., Appaji, N., Yagi, K., 1972. The occurrence of superoxide anion in the reaction of reduced phenazine methosulfate and molecular oxygen. *Biochem. Biophys. Res. Commun.* 46, 849–854. [https://doi.org/10.1016/s0006-291x\(72\)80218-3](https://doi.org/10.1016/s0006-291x(72)80218-3).
- Perše, M., Večerić-Haler, Ž., 2018. Cisplatin-induced rodent model of kidney injury: Characteristics and challenges. *Biomed. Res. Int.* 2018. <https://doi.org/10.1155/2018/1462802>.
- Pınar, N., Topaloğlu, M., Seçinti, I.E., Büyük, E., Kaplan, M., 2022. Protective effect of dexpanthenol on cisplatin induced nephrotoxicity in rats. *Biotech. Histochem. Off. Publ. Biol. Stain Comm.* 97, 39–43. <https://doi.org/10.1080/10520295.2021.1890215>.
- Rafat, A., Mohammadi Roushandeh, A., Alizadeh, A., Hashemi-Firouzi, N., Golipour, Z., 2019. Comparison of the melatonin preconditioning efficacy between bone marrow and adipose-derived mesenchymal stem cells. *Cell J.* 20, 450–458. <https://doi.org/10.22074/cellj.2019.5507>.
- Salehinejad, P., Alitheen, N.B., Ali, A.M., Omar, A.R., Mohit, M., Janzamin, E., Samani, F.S., Torshizi, Z., Nematollahi-Mahani, S.N., 2012. Comparison of different methods for the isolation of mesenchymal stem cells from human umbilical cord Wharton's jelly. *In Vitro Cell. Dev. Biol. Anim.* 48, 75–83. <https://doi.org/10.1007/s11626-011-9480-x>.
- Sun, Z., Xu, S., Cai, Q., Zhou, W., Jiao, X., Bao, M., Yu, X., 2020. Wnt/ β -catenin agonist BIO alleviates cisplatin-induced nephrotoxicity without compromising its efficacy of anti-proliferation in ovarian cancer. *Life Sci.* 263. <https://doi.org/10.1016/j.lfs.2020.118672> 118672.
- Tang, Q., Wang, X., Jin, H., Mi, Y., Liu, L., Dong, M., Chen, Y., Zou, Z., 2021. Cisplatin-induced ototoxicity: Updates on molecular mechanisms and otoprotective strategies. *Eur. J. Pharm. Biopharm. Off. J. Arbeitsgemeinschaft fur Pharm. Verfahrenstechnik e.V.* 163, 60–71. <https://doi.org/10.1016/j.ejpb.2021.03.008>.
- Turgut, O., Ay, A.A., Turgut, H., Ay, A., Kafkas, S., Dost, T., 2013. Effects of melatonin and dexpanthenol on antioxidant parameters when combined with estrogen treatment in ovariectomized rats. *Age (Dordr.)* 35, 2229–2235. <https://doi.org/10.1007/s11357-013-9519-x>.
- Uysal, H.B., Yilmaz, M., Gokcimen, A., 2017. Protective effects of dexpanthenol against acetaminophen-induced hepatorenal damage. *Biomed. Res.* 28, 740–749.
- Wong, C.-Y., 2021. Current advances of stem cell-based therapy for kidney diseases. *World J. Stem Cells* 13, 914–933. <https://doi.org/10.4252/wjsc.v13.i7.914>.
- Yao, W., Hu, Q., Ma, Y., Xiong, W., Wu, T., Cao, J., Wu, D., 2015. Human adipose-derived mesenchymal stem cells repair cisplatin-induced acute kidney injury through antiapoptotic pathways. *Exp. Ther. Med.* 10, 468–476. <https://doi.org/10.3892/etm.2015.2505>.
- Yoon, D.S., Choi, Y., Choi, S.M., Park, K.H., Lee, J.W., 2015. Different effects of resveratrol on early and late passage mesenchymal stem cells through β -catenin regulation. *Biochem. Biophys. Res. Commun.* 467, 1026–1032. <https://doi.org/10.1016/j.bbrc.2015.10.017>.
- Zhang, L., Tan, X., Dong, C., Zou, L., Zhao, H., Zhang, X., Tian, M., Jin, G., 2012. In vitro differentiation of human umbilical cord mesenchymal stem cells (hUCMSCs), derived from Wharton's jelly, into choline acetyltransferase (ChAT)-positive cells. *Int. J. Dev. Neurosci. Off. J. Int. Soc. Dev. Neurosci.* 30, 471–477. <https://doi.org/10.1016/j.ijdevneu.2012.05.006>.
- Zhao, X., Zhang, S., Shao, H., 2022. Dexpanthenol attenuates inflammatory damage and apoptosis in kidney and liver tissues of septic mice. *Bioengineered* 13, 11625–11635. <https://doi.org/10.1080/21655979.2022.2070585>.

Further Reading

- Kızılay, Z., Kahraman Çetin, N., Yaycıoğlu, S., Yay, M.Ö., Öztürk, H., Yenisey, Ç., 2020. The effect of dexpanthenol on the formation of epidural fibrosis in an experimental laminectomy model in rats. *J. Surg. Med.* 4, 16–20. <https://doi.org/10.28982/josam.597612>.